

Electronic Supporting Information (ESI)

Highly Emissive Near-Infrared Solid Organic Fluorophores for Visualization of Latent Fingerprints based on Mobile-Phone Photographing

Zheng Lv, Zhongwei Man, Zhenzhen Xu,* Shuai Li, Qing Liao and Hongbing Fu*

1. Materials and methods

1.1 Materials

All reagents for organic synthesis were commercially available and used as received without further purification. Montmorillonite (MMT) powder was brought from Innochem. Traditional magnetic powders (ferric oxide) and commercial fingerprint powders were purchased from U-MAG Materials Company and Beijing BoNa HengDa Technology, respectively. 405 nm LED lamp (3W) was purchased from ANJOET.

1.2 Methods

1.2.1 Characterization Methods

The compound was confirmed by High resolution mass spectroscopy (GCT-MS Micromass, UK) and ¹H-NMR (400 MHz, 293K). The absorption spectra were recorded by Shimidazu UV-3600 UV-VIS-NIR spectrophotometer and the fluorescence spectra were measured by a FluoroMax-4 (Horiba). The fluorescence lifetimes and quantum yields were measured based on Edinburgh Instrument FLS1000 Integrating sphere.

1.2.2 Preparation of single crystals

CASN and TASN single crystals were obtained by the slow evaporation of the saturated dichloromethane solution at room temperature. IM-1 single crystals were prepared by the solvent diffusion method at the liquid-liquid interface between dichloromethane and petroleum ether solution at room temperature.

1.2.3 Collection of fingerprints

The volunteers were asked to lightly touch their foreheads with their fingers and then pressed their fingers on the different substrate surfaces.

1.2.4 Development of LFPs by powder dusting method.

The 0.2-4 mg TASN were dissolved in dichloromethane (DCM) and 20 mg MMT were added. After sonication for 5 min, the solvent was evaporated by rotary evaporator. The obtained powders were grounded by mortar to completely mix TASN

with MMT. The products were dried in oven for overnight and stored in dry vessels before use. A small amount of fingerprint powders were carefully added on these substrates printed with LFPs for about 5 s. Then excessive powders could be gently blew away by rubber suction bulb .

1.2.5 Image acquisition equipment.

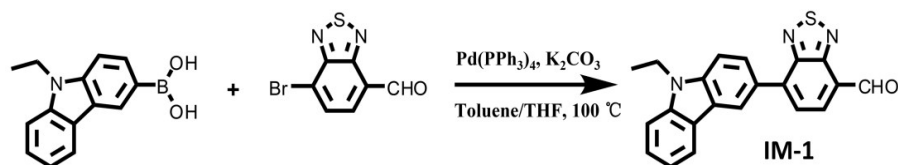
The LFP images were obtained under 405 nm LED lamp (ANJOET-501B, 3W), with an iPhone 6s plus as the signal collector. Grayscale analysis was performed by ImagJ software from the National Institutes of Health (U.S.).

2. General procedure for the synthesis of target compounds

2.1 Synthesis of CASN

Synthesis of IM-1

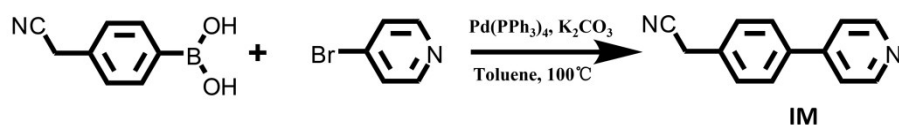
The synthetic method was modified by the reported procedure. ^[S1]



Scheme S1. Synthetic route of IM-1.

Synthesis of IM

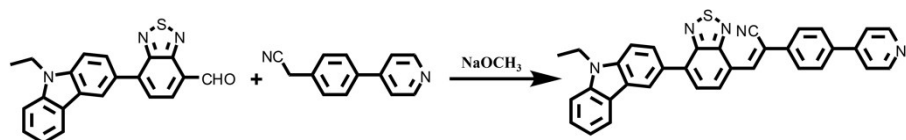
The synthesis of IM was reported in the previous work.¹



Scheme S2. Synthetic route of IM.

Synthesis of CASN

IM-1(0.715 g, 2 mmol), IM (0.388 g, 2 mmol) and a certain amount of NaOCH₃ (0.011g,0.2 mmol) were added in 15 mL ethanol and 10 mL THF. Then the mixture were stirred at room temperature for 12h. The resulting compound was filteres and repeatedly washed with 50 % EtOH aqueous solution to give red powders (0.652 g, 61.2%).

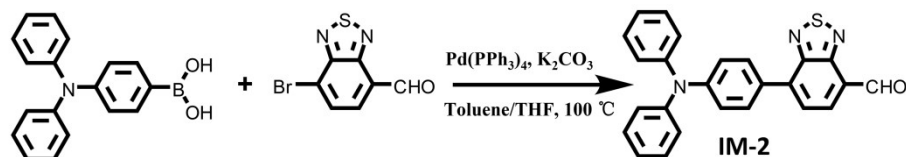


Scheme S3. Synthetic route of CASN.

2.2 Synthesis of TASN

Synthesis of IM-2

The synthetic method was modified by the reported procedure. [S1]



Scheme S4. Synthetic route of IM-2.

Synthesis of IM

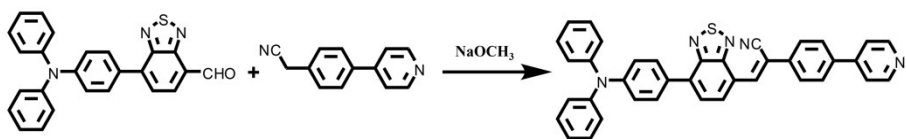
The synthesis of IM was reported in the previous work. [S2]



Scheme S2. Synthetic route of IM.

Synthesis of TASN

IM-2(0.810 g, 2 mmol), IM (0.388 g, 2 mmol) and a certain amount of NaOCH₃ (0.011g,0.2 mmol) were added in 15 mL ethanol and 10 mL THF. Then the mixture were stirred at room temperature for 12h. The resulting compound was filteres and repeatedly washed with 50 % EtOH aqueous solution to give red powders (0.842 g, 72%).



Scheme S3. Synthetic route of TASN.

3. Supplementary figures and tables

Table S1. The reported organic dyes for LFP development

compound	λ_{ex}	λ_{em}	time	medium	reference
TPE	365 nm	~ 440 nm	5 min	CH ₃ CN/H ₂ O	Chem. Commun. 2012, 48, 4109
DPPS-2	365 nm	518 nm	2 min	CH ₃ CN/H ₂ O	J. Mater. Chem. C, 2016, 4, 11180
NIFA	365 nm	525 nm	17 min	Ethanol/H ₂ O	Sens. Actuators, B. 2019, 283, 99
FLA-2	365 nm	525 nm	20 min	CH ₃ CN/H ₂ O	Analyst. 2020, 145, 2311
DPSA	365 nm	564 nm	5 min	CH ₃ CN/H ₂ O	New J. Chem. 2018, 42, 12900
NIR-LP	365 nm	~ 650 nm	20 min	CH ₃ CN/H ₂ O	RSC Adv., 2015, 5, 87306
TPA-1OH	405 nm	658 nm	30 s	H ₂ O	J. Am. Chem. Soc. 2020, 142,7497
BN-9	365 nm	505 nm	30 s	none	Angew. Chem. Int. Ed. 2019, 58, 10132
TPE-4DPA	365 nm	500 nm	none	magnetic powder	Sci China Chem, 2018, 61, 966
SAA	365 nm	550 nm	30 s	montmorillonite	Mater. Chem. Front., 2020,4, 2131
DMAS-TP	365 nm	615 nm	none	silica	J. Mater. Chem. C, 2021
TASN	405 nm	686 nm	10 s	montmorillonite	This work

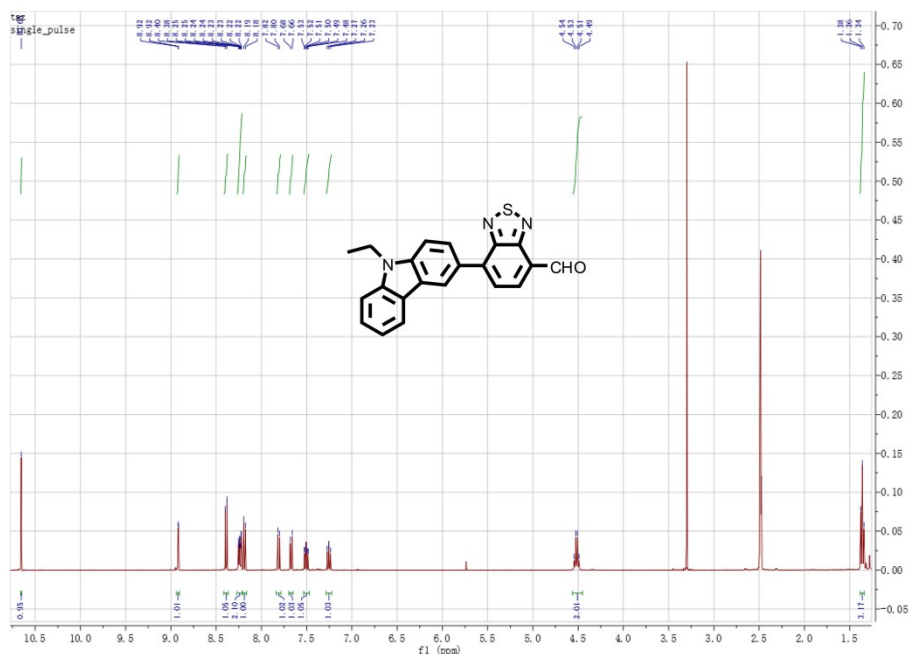


Fig. S1 ¹HNMR spectrum of compound IM-1. ¹HNMR (400 MHz, DMSO-d₆) δ 10.65 (s, 1H), 8.92 (d, J = 1.4 Hz, 1H), 8.39 (d, J = 7.5 Hz, 1H), 8.27 – 8.21 (m, 2H), 8.19 (d, J = 7.3 Hz, 1H), 7.81 (d, J = 8.5 Hz, 1H), 7.67 (d, J = 8.2 Hz, 1H), 7.53 – 7.47 (m, 1H), 7.28 – 7.22 (m, 1H), 4.52 (q, J = 7.1 Hz, 2H), 1.36 (t, J = 7.2 Hz, 3H).

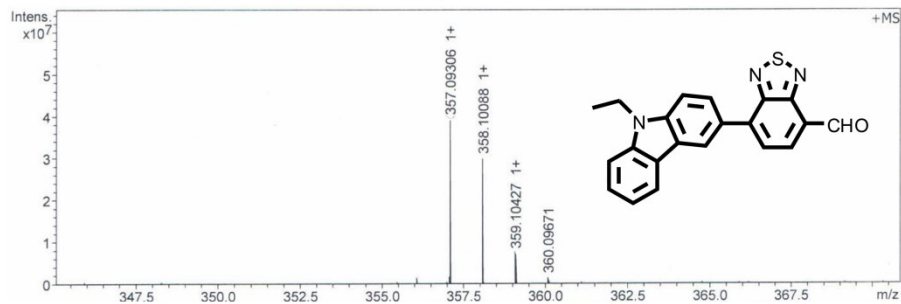


Fig. S2 HR-MS (MALDI-MS) spectrum of IM-1, $m/z = 357$.

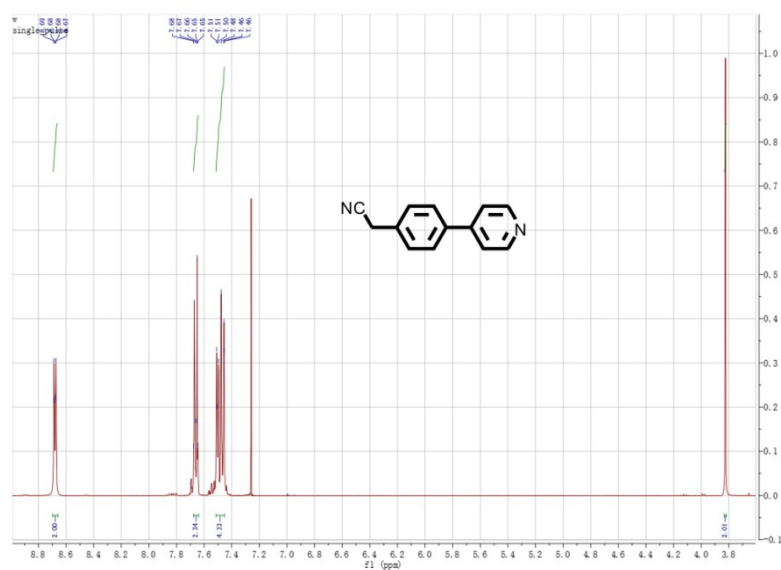


Fig. S3 ^1H NMR (400 MHz, Chloroform- d) δ 8.68 (dd, $J = 4.7, 1.4$ Hz, 2H), 7.68 – 7.64 (m, 2H), 7.51 – 7.45 (m, 4H), 3.82 (s, 2H).

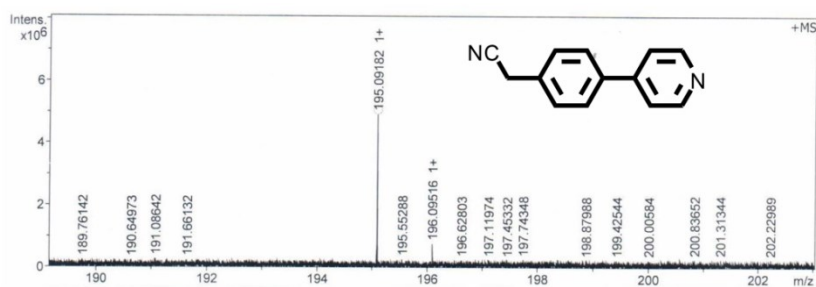


Fig. S4 HR-MS (MALDI-MS) spectrum of IM, $m/z = 194$.

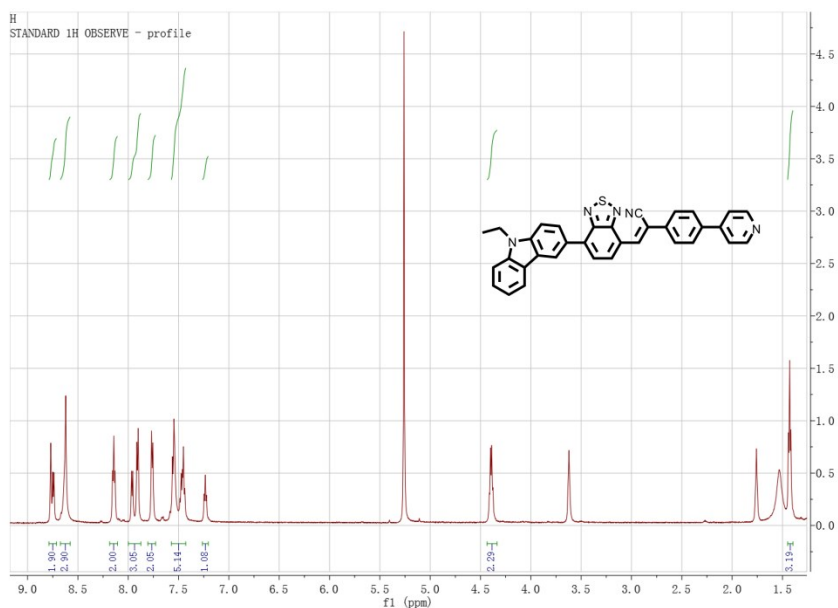


Fig. S5 ^1H NMR (600 MHz, Methylene Chloride- d_2) δ 8.79 – 8.71 (m, 2H), 8.62 (s, 3H), 8.14 (t, $J = 7.4$ Hz, 2H), 7.93 (dd, $J = 31.8, 7.6$ Hz, 3H), 7.76 (d, $J = 7.9$ Hz, 2H), 7.57 – 7.43 (m, 5H), 7.23 (t, $J = 7.2$ Hz, 1H), 4.39 (q, $J = 7.3$ Hz, 2H), 1.43 (t, $J = 7.3$ Hz, 3H).

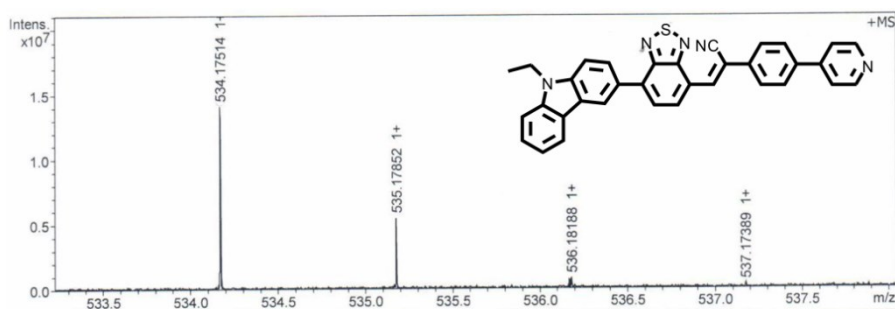


Fig. S6 HR-MS (MALDI-MS) spectrum of CASN, $m/z = 533$.

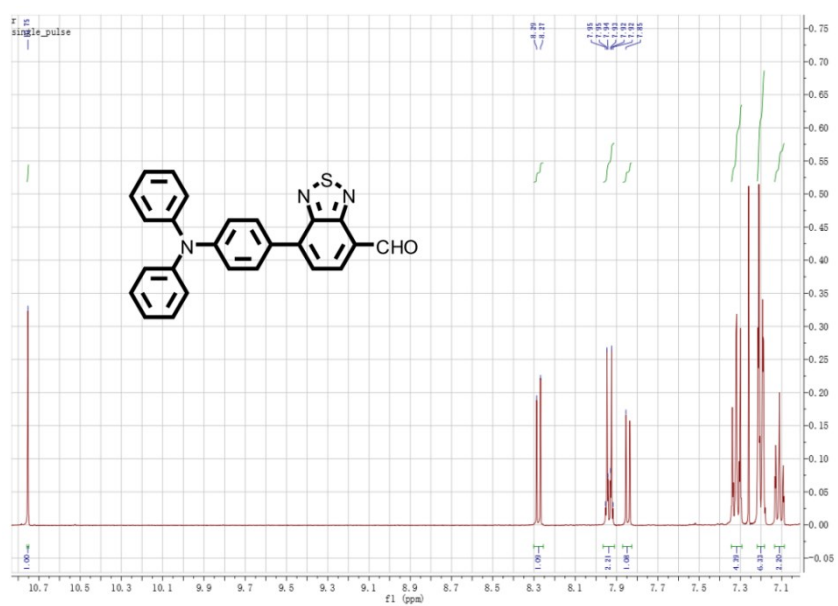


Fig. S7 ^1H NMR (400 MHz, Chloroform- d) δ 10.75 (s, 1H), 8.28 (d, $J = 7.4$ Hz, 1H), 7.96 – 7.91 (m, 2H), 7.85 (s, 1H), 7.32 (s, 4H), 7.21 (d, $J = 1.9$ Hz, 6H), 7.12 (d, $J = 4.9$ Hz, 2H).

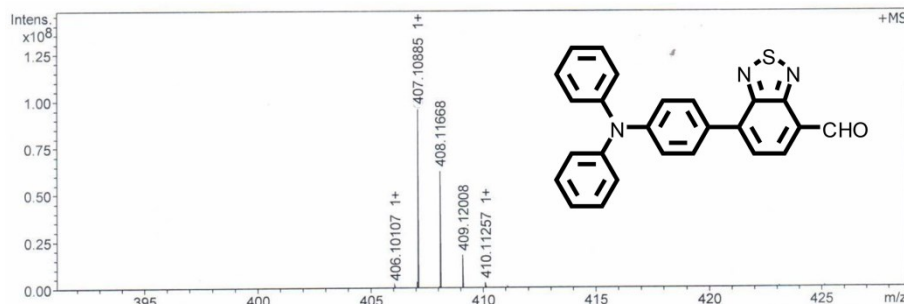


Fig. S8 HR-MS (MALDI-MS) spectrum of IM-2, $m/z = 407$.

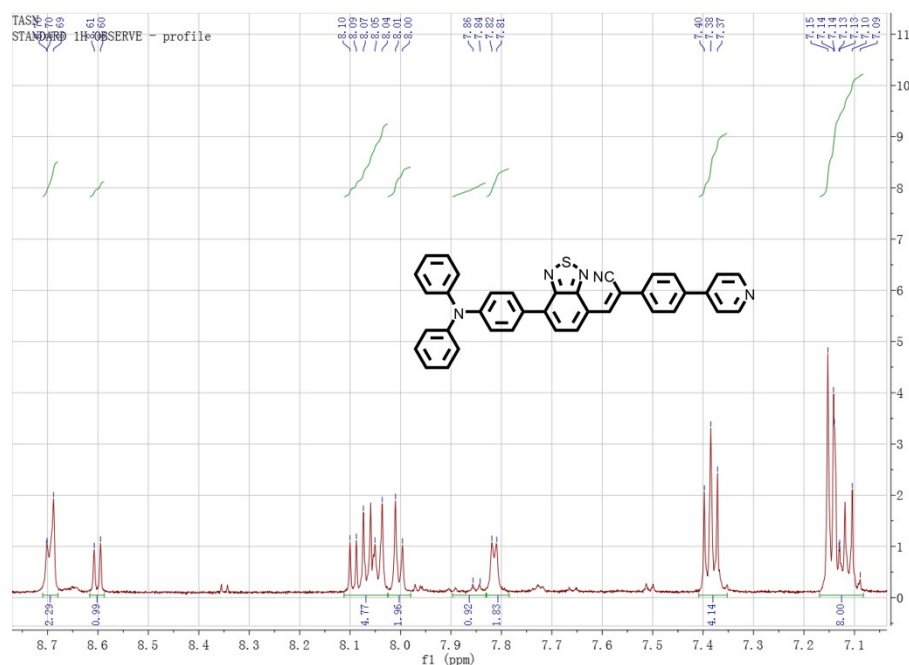


Fig. S9 ^1H NMR (600 MHz, DMSO- d_6) δ 8.71 – 8.68 (m, 2H), 8.60 (d, $J = 7.4$ Hz, 1H), 8.11 – 8.03 (m, 5H), 8.00 (d, $J = 8.4$ Hz, 2H), 7.85 (d, $J = 8.5$ Hz, 1H), 7.81 (d, $J = 5.8$ Hz, 2H), 7.41 – 7.35 (m, 4H), 7.17 – 7.08 (m, 8H).

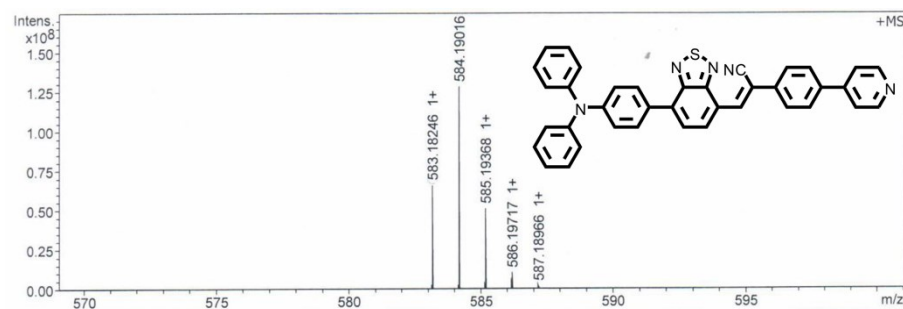


Fig. S10 HR-MS (MALDI-MS) spectrum of TASN, $m/z = 583$.

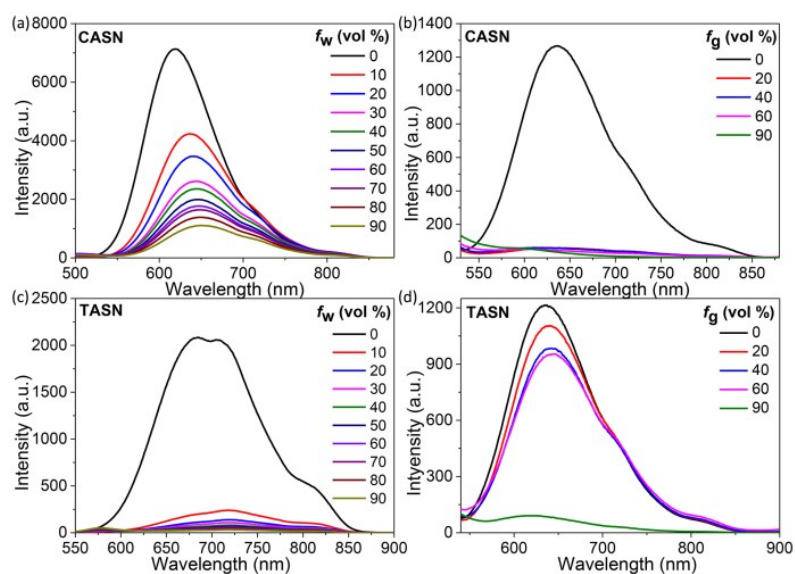


Fig. S11 The emission spectra of (a) CASN and (c) TASN in mixtures of THF-water with different water fractions (f_w). The emission spectra of (b) CASN and (d) TASN in mixtures of ethanol-glycerol with different glycerol fractions (f_g).

Notes: We have performed the AIE tests of CASN and TASN. CASN and TASN were first dissolved in THF solution, respectively. The emission intensities gradually decreased after addition of a poor solvent of water with different fractions into its THF solution. Moreover, the emission intensities gradually decreased after addition of glycerin with different fractions into its ethanol solution. These results indicated that CASN and TASN didn't exhibit typical AIE characteristic. Hence, CASN and TASN are not AIE-active fluorophores.

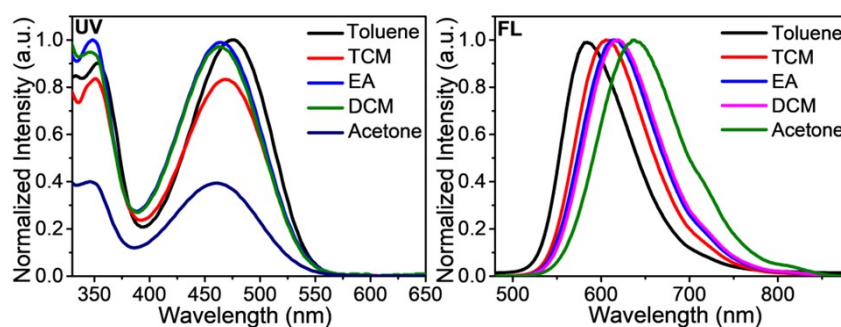


Fig. S12 The UV absorption spectra and FL emission spectra of CASN, measured in the different solvents with increasing polarity.

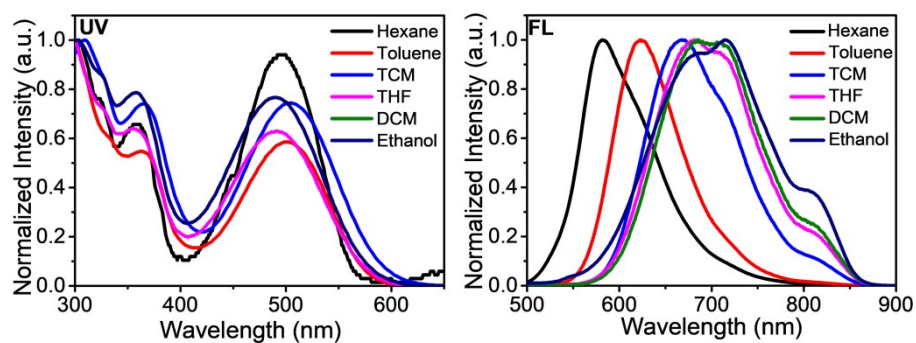


Fig. S13 The UV absorption spectra and FL emission spectra of TASN, measured in the different solvents with increasing polarity.

Table S2. Detailed photo-physical data of CASN and TASN in the different solvents

	solvent	Δf	ϵ $L^*mol^{-1}cm^{-1}$	λ_{abs} (nm)	λ_{em} (nm)	Stokes' Shift(nm)	Φ	τ (ns)	k_r (ns^{-1})	k_{nr} (ns^{-1})
CASN	Toluene	0.018	35140	475	584	109	0.838	3.71	0.226	0.044
	TCM	0.145	27428	468	605	137	0.591	3.31	0.178	0.123
	EA	0.200	12780	464	616	152	0.512	3.41	0.159	0.134
	DCM	0.218	42306	462	618	156	0.507	3.37	0.150	0.146
	Acetone	0.284	23469	460	637	177	0.334	4.04	0.083	0.164
TASN	Toluene	0.018	21000	503	623	120	0.990	4.36	0.227	0.023
	TCM	0.145	22120	504	668	164	0.699	4.94	0.141	0.061
	THF	0.211	26050	491	682	191	0.391	2.94	0.133	0.210
	DCM	0.218	11350	491	686	195	0.310	2.81	0.110	0.250
	Ethanol	0.288	26000	490	715	225	0.077	2.94	0.026	0.313

Table S3. Summary of the single crystals data of IM-1, CASN and TASN.

	IM-1	CASN	TASN
CCDC	205362	2048593	2048597
Crystal system	Triclinic	Triclinic	Triclinic
Space group	P-1	P-1	P-1
$a/\text{\AA}$	12.1454(2)	10.3589(3)	8.9522(6)
$b/\text{\AA}$	19.0331(2)	11.2429(2)	11.9366(9)
$c/\text{\AA}$	22.7194(3)	23.5516(7)	13.9351(10)
$\alpha/^\circ$	95.0070(10)	89.688(2)	92.148(6)
$\beta/^\circ$	97.8220(10)	78.968(2)	91.879(6)

$\gamma/^\circ$	106.8050(10)	87.836(2)	102.640(6)
$v/\text{\AA}^3$	4936.26(12)	2690.30(12)	1450.69(18)
Z Value	12	4	2
$v/z/\text{\AA}^3$	411.35	672.575	725.345
$\rho_{calc}/\text{g cm}^{-3}$	1.870	1.317	1.336
Final R indexes [$I \geq 2\sigma$ (I)]	$R_1 = 0.0566,$ $wR_2 = 0.2062$	$R_1 = 0.0409,$ $wR_2 = 0.1075$	$R_1 = 0.0505,$ $wR_2 = 0.1132$
Final R indexes [all data]	$R_1 = 0.0915,$ $wR_2 = 0.2572$	$R_1 = 0.0505,$ $wR_2 = 0.1157$	$R_1 = 0.0695,$ $wR_2 = 0.1255$
GOF	0.885	1.031	1.042

Table S4. Summarization of weak interactions in the crystals of CASN and TASN.

CASN	Interactions	d/\AA
1	C3 H24	2.675
2	N4 N8	3.066
3	N4 C51	3.142
4	C21 H44	2.730
5	C7 H26	2.705
6	C8 H26	2.886
7	S1 N7	2.971
8	S1 C45	3.292
9	N3 S2	3.296
10	N3 N7	3.090
11	C37 H60	2.844
12	C38 H59	2.866
13	C48 H59	2.792

14	N9 H53	2.693
15	C40 H68	2.807
TASN	Interactions	d/Å
1	H37 C30	2.913
2	N2 H26	2.863
3	C38 H21	2.881

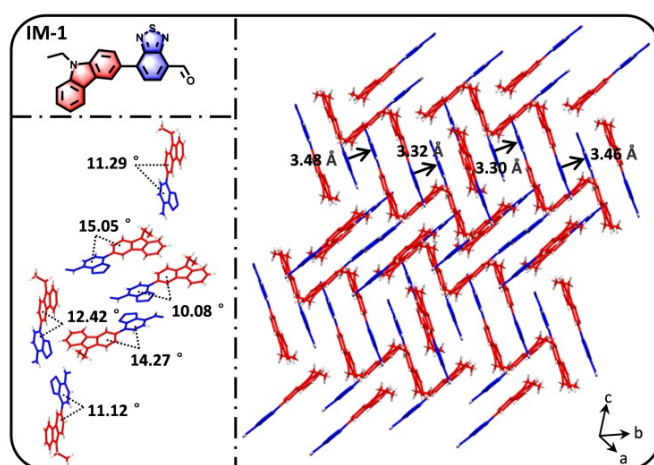


Fig. S14 The molecular structure of IM-1 (intermediate of CASN) and its illustration of crystal packing as well as intermolecular interaction.

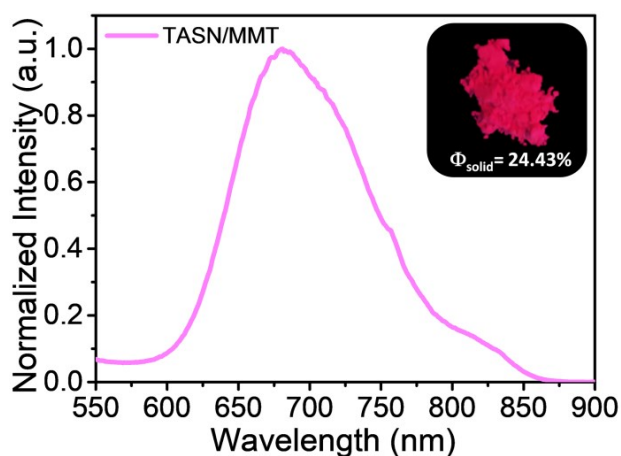


Fig. S15 Emission spectrum and photographs of TASN/MMT powder ($f_{\text{TASN}} = 10\%$) under 365 nm UV excitation, including solid-state quantum yield (Φ_{solid}).

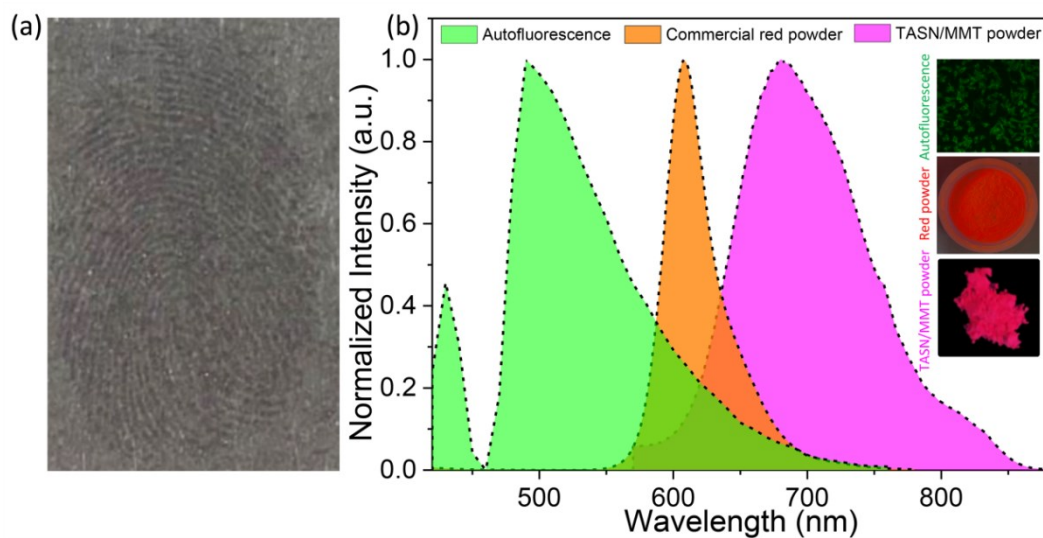


Fig. S16 (a) LFP imaging of magnetic powder. (b) The emission spectra of auto-fluorescence with macrophages, commercial red powder and TASN/MMT powder. Inset: the corresponding fluorescent images.

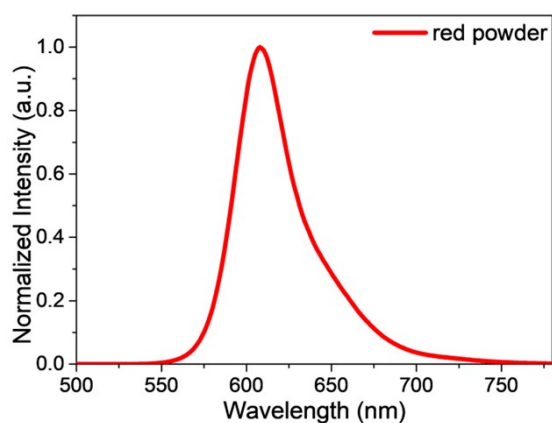


Fig. S17 The emission spectrum of commercial red fingerprint powder in solid state.

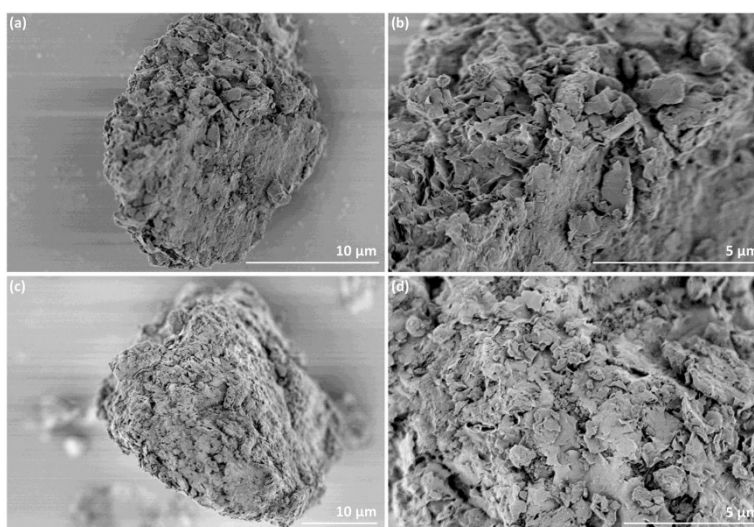


Fig. S18 SEM images of (a-b) MMT powders and (c-d) TASN/MMT composite powders.

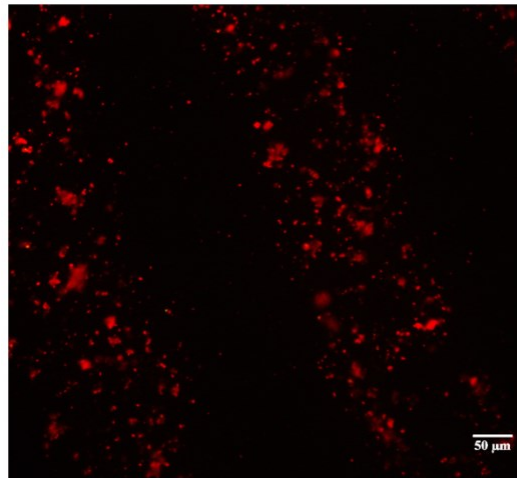


Fig. S19 Fluorescence image of the developed LFP. The scale bar is 50 μm.

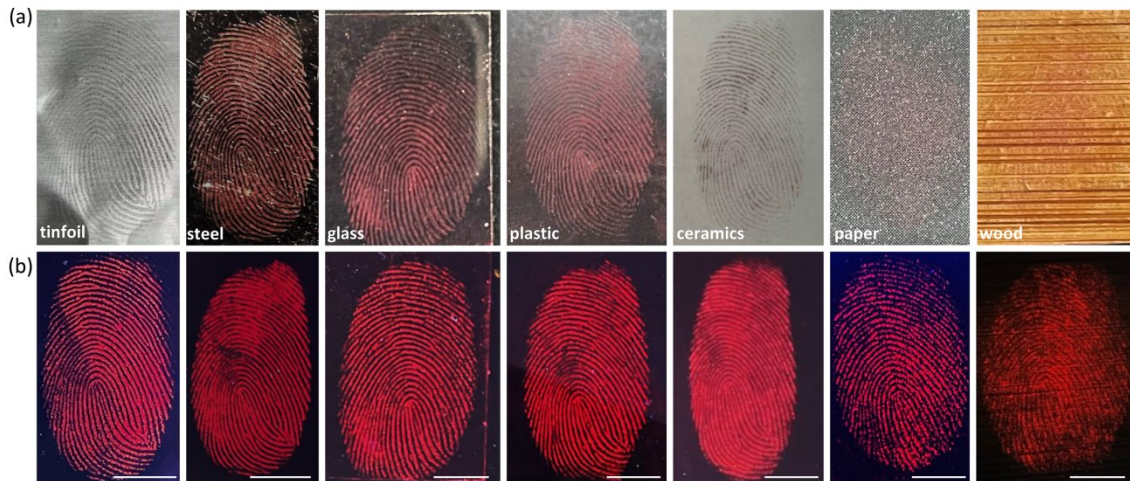


Fig. S20 Fingerprints stained with TASN/MTT powder under (a) white light and (b) 405 nm irradiation. The scale bar is 0.5 mm.

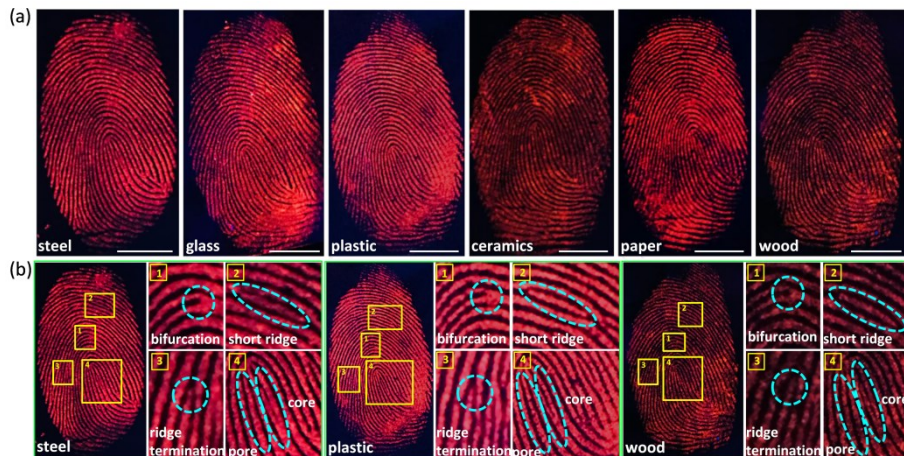


Fig. S21 RGB true-color photographs (under 405 nm irradiation) of whole LFPs on different substrates were developed by TASN/MMT powders. (b) Level 1, level 2, and level 3 details of local LFPs on steel, plastic, and wood developed by TASN/MMT powders. The scale bars are 0.5 mm.

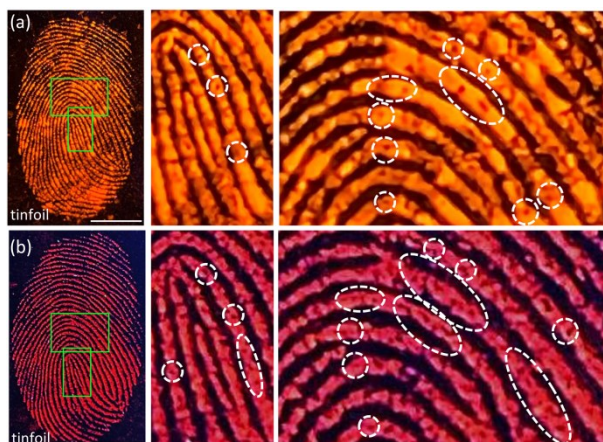


Fig. S22 Fluorescence images about level 3 details of LFP on tinfoil developed with (a) commercial red fingerprint powder and (b) TASN/MTT powder under the excitation of 405 nm light.

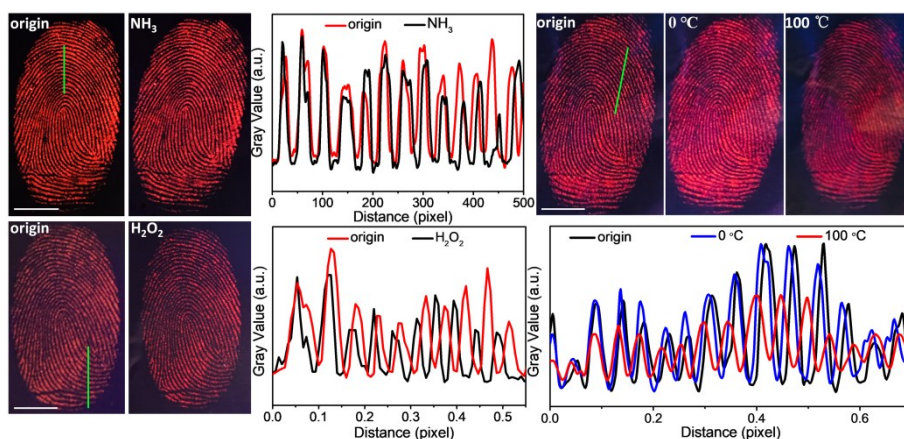


Fig. S23 Photographs of latent fingerprints developed with TASN/MMT powders on glass slide before and after abrasion with low/high temperature, hydrogen peroxide and ammonia treatment. The scale bars are 0.5 mm.

4. References

- [1] a) C. Lv, W. Liu, Q. Luo, H. Yi, H. Yu, Z. Yang, B. Zou, Y. Zhang, *Chem.Sci.* **2020**, *11*, 4007-4015; b) Q. Luo, L. Li, H. Ma, C. Lv, X. Jiang, X. Gu, Z. An, B. Zou, C. Zhang, Y. Zhang, *Chem. Sci.* **2020**, *11*, 6020-6025.
- [2] A. Labrunie, Y. Jiang, F. Baert, A. Leliège, J. Roncali, C. Cabanetos, P. Blanchard, *RSC Adv.* **2015**, *5*, 102550-102554.